Particle-Rotor Model Study of the Transitional N = 89 and Some N = 91-95 Nuclei



1979 Phys. Scr. 19 497

(http://iopscience.iop.org/1402-4896/19/5-6/002)

Physica Scripta. Vol. 19, 497–508, 1979

# Particle-Rotor Model Study of the Transitional N = 89 and Some N = 91–95 Nuclei

R. Katajanheimo

Department of Physics, University of Helsinki, Helsinki, Finland

and

E. Hammarén

Department of Physics, University of Jyväskylä, Jyväskylä, Finland

*Received September 4, 1978; final version November 11, 1978*

## Abstract

*Particle-rotor model study of the transitional $N = 89$ and some $N = 91-95$ nuclei. R. Katajanheimo (Department of Physics, University of Helsinki, Helsinki, Finland); and E. Hammarén (Department of Physics, University of Jyväskylä, Jyväskylä, Finland).*
*Physica Scripta (Sweden) 19,* 497–508, 1979.

A particle-rotor model with a nonspheroidal axial and reflection symmetric Woods–Saxon potential has been used to describe the rotational bands and gamma branching ratios in some odd-mass nuclei with 95 to 89 neutrons. Systematics of the deformation parameters have been found by calculations in the well-deformed region. The model is capable of giving a systematic classification of the low-lying odd-parity excitations in the $N = 91$ and expecially in the $N = 89$ nuclei. An important result is the identification of the $\frac{7}{2}^+$, $\frac{3}{2}^+$ and $\frac{5}{2}^+$ members of the $\frac{3}{2}^+[651]$ side band in the weakly deformed nuclei. These discoveries also provide a reliable foundation for the classification of other low-spin states.

## 1. Introduction

During recent years experimental information on the $N = 89$–$95$ nuclei has increased remarkably. The growth has been most rapid for the $N = 89$ nuclei [1–12], which has prompted theoretical attempts to describe the structure of these nuclei with particle-rotor models. Calculations for the odd- and even-parity states of $^{155}$Dy [1, 2] and $^{153}$Gd [5, 13], respectively, have been performed with various versions of the conventional Nilsson model [14, 15], which have been used to describe the even-parity bands of $^{151}$Sm [9] and $^{149}$Nd [11] as well. The even-parity states of $^{155}$Dy have also been examined with a model including a variable moment of inertia [16]. In addition, a promising calculation [17] to classify the odd-parity states of $^{151}$Sm into rotational bands has been made with an extended Nilsson model [18]. However, in all of those calculations the positive- and negative-parity states of a particular nucleus have been considered independently of each other.

According to our present knowledge, rotational motion may be responsible for the existence of most of the low-energy excitations in the $N = 89$ isotones. Thus one can expect that a particle-rotor model with a realistic Woods–Saxon potential [19, 20] can be used to explain some previously poorly understood features of all the nuclei under consideration. As the model apparently includes a large number of free parameters, we have used spherical and well-known deformed nuclei in order to find out the parameter systematics. An obvious advantage, and at the same time a remarkable difficulty of the model, is that the resulting energies give excitations relative to the real ground state both for even- and for odd-parity bands. As a further test of the validity of the model we have used the predicted gamma branching ratios, since the lifetimes are known only for an insignificant number of the states considered.

On the basis of the deduced systematics, combined with model predictions, we have succeeded in giving a clear systematic description of the previously ambiguous odd-parity states in all the $N = 89$ nuclei. In particular, of the two earlier contradictory assignments for the ground bands of $^{155}$Dy and $^{153}$Gd, we have been able to select the $\frac{3}{2}^-[521]$ band. Both of these results require, however, that we have shifted one or two of the six strongly interacting low-lying band heads to their experimental energies separately in every particular nucleus.

Hjorth and Klamra [16] have stated recently that the structure of the low-spin even-parity states is poorly understood, at least in transitional nuclei. Thus only the high-spin members of the decoupled $\frac{1}{2}^+[660]$ band are well described by the particle-rotor models applied. The present study has increased the knowledge about all of these low-spin states considerably, although the main object has been the $\frac{3}{2}^+[651]$ side band. The previously fully unknown $\frac{7}{2}^+$ member, as well as the band head and the $\frac{5}{2}$ member of this band, have been identified in $^{155}$Dy and $^{153}$Gd. We discuss the properties of these states together with the corresponding ones in $^{151}$Sm, where the high-spin members of this side band have been identified, too.

We would like to emphasize, however, that the present tentative assignments especially those, which obviously differ from the previous ones, are often based on rather small number of experimental data. Therefore an alternative single-particle assignment can be as probable as given here. In addition a possibility of vibrational or three-quasi-particle character of the intrinsic excitations has been omitted in the spirit of the model description. Consequently the decay- and population properties of the $\frac{1}{2}^-[521]$ band members are interpreted successfully without making the assumption that they may have vibrational nature.

In the next section the model, the choice of parameter values and the reduction of the Coriolis and recoil terms are discussed. The results of the calculations are compared with experiments separately for each isotonic row under consideration in Section 3. The main results are summarized in Table V.

## 2. A review of the model

A detailed and comprehensive description of the particle-rotor model used in the present calculations has been given

by Wahlborn and co-workers [19, 20]. We shall repeat briefly the main ideas of the model, and concentrate on describing the selection of the various parameters and the limitations in the numerical analysis. In the original Hamiltonian [20] we have included two additional assumptions: (i) a reduction of the Coriolis and recoil terms [see eq. (4)] and (ii) a possibility to change the single-particle level density near the Fermi surface. The reasons for these alterations and their consequences are discussed in Subsections 2.2 and 2.4.

### 2.1. *The model Hamiltonian*

The model Hamiltonian which includes the particle motion and the collective rotation of a nucleus can be written in the form

$$H_{\mathrm{mod}} = H_{\mathrm{qp}} + H_{\mathrm{qprot}} \tag{1}$$

The total energy of the intrinsic quasiparticle system is a sum of the single-particle energies and the total pairing contribution,

$$H_{\mathrm{qp}} = \sum_{\nu} \epsilon_\nu a_\nu^+ a_\nu - G \sum_{\nu\nu'} a_{-\nu}^+ a_{\nu'}^+ a_\nu a_{-\nu'} \tag{2}$$

Here we use the familiar occupation number representation and the constant-force BCS approximation for pairing [19, 20]. The summations run over the neutron states only, i.e., we omit the possible but weak neutron–proton interaction. The single-particle energies $\epsilon_\nu$ for neutron orbitals are eigenvalues of the Hamiltonian [20]

$$H_{\mathrm{ws}} = T + V(r) + V_{\mathrm{s0}}(r, \mathrm{spin}), \tag{3}$$

which is based on nonspheroidal Woods–Saxon potentials.

The rotational part of eq. (1) is usually divided into three different contributions,

$$H_{\mathrm{qprot}} = H_I + kH_{\mathrm{RPC}} + k^2 H_j \tag{4}$$

Here we explicitly indicate the extra reduction factors which are added to the original particle-rotor scheme [20]. By means of the familiar angular momentum operators and strong-coupling assumption the different terms in eq. (4) are

$$H_I = A(I^2 - I_z^2), \quad A = \hbar^2/2J, \tag{5}$$

$$H_{\mathrm{RPC}} = -A(I_+ j_- + I_- j_+), \tag{6}$$

$$H_j = A(\mathrm{j}^2 - j_z^2). \tag{7}$$

The diagonalization of the various parts of the Hamiltonian (1) will be discussed in Subsection 2.3.

### 2.2. *Parametrization*

In principle, the single-particle Hamiltonian $H_{\mathrm{ws}}$ of eq. (3) contains nine parameters in all. Six of them can be classified as the so-called potential parameters $\{r_0, a_\perp, a_z\}$, which are well-defined [21, 22] for both of the two potential terms in eq. (3). Thus the only really free parameters are the potential depths $V_0$ and the spin–orbit strength $\lambda$. In fixing these parameters we follow the method of Batty and Greenlees [22]. Accordingly the values are chosen to give the best fit to the experimental single-particle levels of the spherical $^{208}$Pb and $^{40}$Ca nuclei. With the recommended parameters $V_0 = 40$ MeV and $\lambda = 30$ our fit for $^{208}$Pb deviates, however, from that given in ref. [22] so that the order of the $4s_{1/2}$ and $2g_{7/2}$ levels is interchanged.

As the diffuseness of all the potential surfaces is kept constant, $a_\perp = a_z = a$, the fitted values of the potential parameters are

$$\begin{aligned} r_0 &= 1.36\,\mathrm{fm} \qquad a = 0.73\,\mathrm{fm} \\ r_{\mathrm{s0}} &= 1.26\,\mathrm{fm} \quad a_{\mathrm{s0}} = 0.60\,\mathrm{fm} \end{aligned} \tag{8}$$

By varying the parameters $V_0$ and $\lambda$ within the limits given in [22] we have checked the validity of the standard parameters (8) also for $^{48}$Ca, where the correct level order and acceptable level spacings were achieved.

According to Almberger et al. [23] the most reliable values of $V_0$ and $\lambda$ for well-deformed rare-earth nuclei are

$$V_0 = 40\,\mathrm{MeV}, \quad \lambda = 32 \tag{9}$$

which values we have applied. Recently some experimental estimates [17, 24] have also been given for the energies of the single-particle states near the $N = 82$ subshell. We are not able, however, to reproduce the scheme presented with the parameters (9). In particular, the energy difference between the $f_{7/2}$ and $h_{9/2}$ states is about 1 MeV too small. This situation may in part explain the observed difficulties in describing the odd-parity states of the $N = 89$ nuclei by the present model.

The starting values for the deformation parameters $\epsilon_2$ and $\epsilon_4$ are taken from the equilibrium deformation contours of Ragnarsson et al. [25]. These curves have been calculated for the even nuclei by using a harmonic oscillator potential. The results are, however, in agreement with the Woods–Saxon calculations of Götz et al. [26]. We have estimated the deformations $\eta_2$ and $\eta_4$ from the curves of [25] by using the relationships

$$\eta_2 = 4/3\epsilon_2, \tag{10a}$$

$$\eta_4 = \epsilon_4 \tag{10b}$$

The model definitions [20] demand a relationship $\eta_4 \approx 2\epsilon_4$ instead of our formula (10b), which arose from a desire to reproduce the previously suggested low-spin positive-parity states and their experimental energies especially in the $N = 89$ nuclei (cf. the later discussion and Table V). The difference between these two choices is, however, significant only for the nuclei where the equilibrium estimates for $\epsilon_4$ are relatively large (see Table I).

In actual calculations the parameter $\eta_2$ is varied within reasonable limits (± 10%) around its equilibrium estimate [25] until one reaches a satisfactory agreement with the observed nuclear properties. The very rapid change in the values of $\eta_2$ (see Table I) when one goes from the neutron number 91 to 89 could have the explanation that the latter nuclei have a hole in the $f_{7/2}$ shell and therefore their deformations are closer to those of the $N = 88$ nuclei. Compare the corresponding discussion of Guttormsen et al. [17].

In addition to the deformation parameters, the model contains only two free parameters for an individual nucleus: the

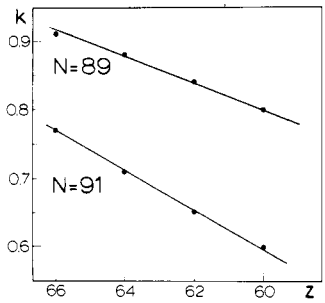


*Fig. 1.* Behaviour of the fitted Coriolis attenuation factor $k$ as a function of proton number $Z$.

Table I. *A compilation of the parameters used in the calculations. The deformation parameters $\eta_2$ and $\eta_4$ correspond to the equilibrium deformations of [25] (cf. Subsection 2.2). The parameters A and k for a particular nucleus are fixed as explained in the text. The transition probabilities have been calculated with the parameters $g_s = 0.6 g_{s\text{free}}$, $g_R = 0.30$–$0.32$, $e_{eff} \simeq (1 - Z/A)e$. If not experimentally known, the quadrupole moments correspond roughly to the quadrupole deformation.*

| | $\eta_2$ | $\eta_4$ | $\Delta_{exp}$ (keV) | $G$ (keV) | $A$ (keV) | $k$ | $N=4^a$ (MeV) | $\frac{11}{2}^-[505]^b$ (MeV) | $Q_0$ (barn) |
|---|---|---|---|---|---|---|---|---|---|
| $^{163}$Er | 0.30 | −0.0 | 1064 | 114 | 13.0 | 0.75 | 1.3 | 0.7 | 7.0 |
| $^{161}$Dy | 0.31 | −0.01 | 968 | 113 | 11.5 | 0.64 | 1.1 | 0.5 | 6.58[c] |
| $^{161}$Er | 0.30 | −0.01 | 1065 | 116 | 14.5 | 0.83 | 1.1 | 0.4 | 6.8 |
| $^{157}$Gd | 0.33 | −0.04 | 932 | 115 | 11.5 | 0.63 | 0.5 | – | 7.0 |
| $^{157}$Dy | 0.30 | −0.02 | 1138 | 121 | 14.5 | 0.77 | 0.8 | 0.2 | 6.1[c] |
| $^{155}$Gd | 0.30 | −0.03 | 1074 | 117 | 13.0 | 0.71 | 0.9 | 0.3 | 6.85[c] |
| $^{153}$Sm | 0.305 | −0.05 | 1128 | 124 | 12.5 | 0.65 | 0.6 | 0.1 | 6.5 |
| $^{151}$Nd | 0.30 | −0.05 | 1010 | 124 | 12.0 | 0.60 | 0.3 | – | 6.5 |
| $^{155}$Dy | 0.18 | −0.023 | 1276 | 126 | 19.0 | 0.91 | 1.8 | 1.3 | 4.55[c] |
| $^{153}$Gd | 0.19 | −0.025 | 1070 | 114 | 18.0 | 0.88 | 2.1 | 1.7 | 4.0 |
| $^{151}$Sm | 0.165 | −0.038 | 1267 | 122 | 19.0 | 0.84 | 2.3 | 1.9 | 3.6 |
| $^{149}$Nd | 0.13 | −0.05 | 1145 | 125 | 19.0 | 0.80 | 2.0 | 1.7 | 3.6 |

[a] The energy shifts applied to the $\frac{3}{2}^+[402]$ and $\frac{1}{2}^+[400]$ hole states.
[b] The same for the $\frac{11}{2}^-[505]$ hole state.
[c] Experimental values.

rotational parameter $A$, eqs. (5)–(7), and the reduction factor $k$, eq. (4) both of which are kept constant for all rotational bands. The parameter $A$ is fixed to reproduce the level spacing within the low-spin members of the pure odd-parity bands, and the reduction factor $k$ to reproduce the experimentally known coupling between the $i_{13/2}$ even-parity states as accurately as possible with the already fixed $A$. In the $N = 89$ nuclei, however, both these parameters are fitted simultaneously to the well-established $I + \frac{1}{2}$ odd rotational states of the decoupled $\frac{1}{2}^+[660]$ band (see Table I and cf. the previous values 0.65 and 1.0 of $k$ for even- and odd-parity states [9, 17] in $^{151}$Sm, respectively).

Traditionally the attenuation factor $k$ has been attached to the Coriolis Hamiltonian $H_{RPC}$ only, since in the Nilsson model the recoil term $H_j$ has been included in the intrinsic Hamiltonian ($H_j \propto \kappa\mu^{l^2}$). Thus the possibly necessary reduction of $H_j$ is partly hidden in the model parameters $\kappa$ and $\mu$. The explicit equations of $H_j$ [20] consist of products of the intrinsic operators $j_+$ and $j_-$. Thus a natural and in this connection consistent way to take into account the reduction necessitated by the existence of high-$j$ even-parity states as ground state is to multiply the operator $H_j$ by the factor $k^2$. This method for reducing the coupling between the intrinsic and collective Hamiltonian can perhaps be viewed as a semi-empirical approximation to the microscopic picture presented by Baznat et al. [27]. In practice this reduction of the recoil term gives a useful 50–100 keV displacement to the band-head energies of the even-parity $i_{13/2}$ states relative to the odd-parity states (see for example the $\frac{5}{2}^+[642]$ states in the $N = 95$ nuclei). A similar recoil-term reduction has been reported in odd Ho isotopes by Nielsen and Bunker [28]. For the other odd-proton nuclei in the same region, the reduction caused a poorer agreement, however. We shall discuss this reduction in more detail for the $N = 95$ nuclei.

### 2.3. *Diagonalization of the model Hamiltonian*

The diagonalization of the single-particle Hamiltonian $H_{ws}$, eq. (3), is done in the basis of harmonic oscillator wave functions expressed in cylindrical coordinates [19, 20]. All eigenfunctions of the oscillator with major quantum number $N \leqslant 13$ are included. The resulting single-particle energies $\epsilon_\nu$, eigenfunctions $\psi_\nu$ and all the single-particle matrix elements contain thus contributions from the $\Delta N = 2$ coupling.

The eigenvalues and eigenvectors of the Hamiltonian $H_{qp}$, eq. (2), are calculated by applying the blocked BCS method [19] to the single-particle energy distribution $\{\epsilon_\nu\}$. In the set $\{\epsilon_\nu\}$ we include approximately 50 states, so that on both sides of the Fermi surface $\lambda^*$ there lie about equal number of single-particle states. The Fermi energy $\lambda^*$ is determined by requiring that the expectation value of the particle number operator coincide with the actual odd number of neutrons. The pairing interaction strength $G$, in turn, is determined by comparing the unblocked energy-gap parameter $\Delta_*$ with the experimental odd–even mass difference $\Delta_{exp}$ (see Table I), which is estimated from the binding energies of the four nearest neighbours [29] by interpolation. As the result of the BCS procedure described we obtain the quasiparticle excitation energies and the corresponding blocked BCS wave functions. They are used to calculate the factors $P_\pm$ and the quasiparticle parts of the operator $H_j$ [20]. We have verified the complete agreement between two approximations [20] and [18] used for the diagonal parts of $H_j$. However, the nondiagonal contributions deviate slightly from each other. This may arise from the spurious effects of the particle number fluctuation [30] in the blocked BCS solution. The small differences, however, do not seriously influence the final results, since the quasiparticle states connected by a large $H_j$ matrix element are as a rule far from each other.

A natural basis for the final diagonalization of the model Hamiltonian (1) consists of the symmetrized eigenfunctions of the adiabatic rigid rotor [20]. The diaonalizations are performed for all the rotational excitations (typically $I \leqslant 21/2$) of the experimentally well-known single-particle states and for the states which mix with the latter.

### 2.4. *Adjustment of some single-particle energies*

With our selection of the various model parameters (cf. Table I) the energies of the even-parity $N = 4$ states and of the state

$\frac{11}{2}^-[505]$ do not correspond the experimental observations. In most calculations performed with the conventional Nilsson model the standard technique to avoid this difficulty has been simply to shift the $\frac{3}{2}^+[402]$ and $\frac{1}{2}^+[400]$ states to the experimental excitations. We have applied this method also to the $\frac{11}{2}^-[505]$ band head. All the shifts made are listed in Table I. These displacements increase the level density below the Fermi surface, which may strongly affect the occupation amplitudes of the individual levels.

As the single-particle matrix elements of the shifted states are calculated clearly with wrong parameters relative to the experimental situation, we have not used the predicted gamma branching ratios for the identification of the indicated states. Fortunately the classification of these levels is usually unambiguous from the available direct reaction data. For all the other rotational states the single-particle matrix elements, which make the crucial contribution to the calculated branching ratios or to the absolute transition probabilities, correspond to the deformations given in Table I.

One unfortunate exception is the interesting $\Delta N = 2$ interaction between the state pair $\frac{3}{2}^+[402] - \frac{3}{2}^+[651]$. Although they appear at the experimental positions after the displacement of the former state, the original single-particle wave functions are too pure to explain their observed decay properties (cf. the discussion of the $N = 93$ nuclei).

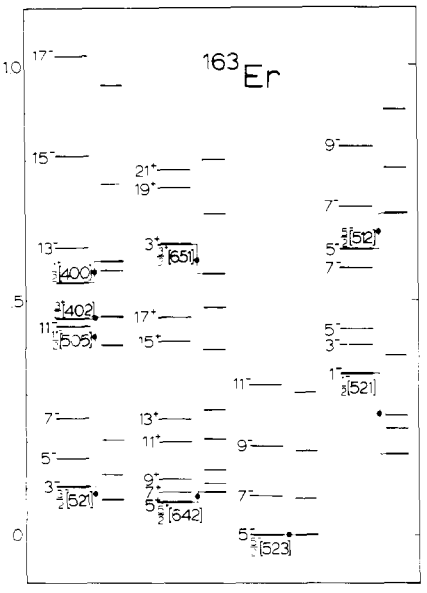


*Fig. 2.* Comparison between the experimental and calculated partial level schemes of $^{163}$Er (energy scale in MeV). The longer lines represent the experimental level energies and the bold ones refer to the band heads, to which assignments are also given. If the experimental band head is unknown, the assignment is marked for the calculated one. The experimental and calculated band heads are connected by lines with a black dot. The spin of each level is given in units of $\hbar/2$. The rotational bands of hole states are displayed on the left and those of particle states on the right of the ground band. The explanations given here are valid for Figs. 3–11.

## 3. Experimental and calculated level schemes

The identification of the rotational bands or individual band heads is based on all available experimental information, which has been collected from various reaction studies and from latest decay scheme works. The experimental levels and their Nilsson-model assignments have been taken from Nuclear Data Sheets or from special references mentioned separately. However, in the cases where our calculations give an obviously different level assignment from the previous one, we shall use the present one. A crude deadline for data collection has been the end of the year 1977. One has to emphasize that our reference list is far from complete, as the tendency has been to mention only the articles most reliable for the present purpose.

As the number of the nuclei studied is quite large, we are forced to restrict the discussion to the common features of nuclei with the same neutron number and to the trends especially interesting with respect to the present model. In this spirit some well-established band heads or hole bands are not discussed in the text at all, though they are shown in the figures. As an example we mention the $\frac{1}{2}^+[400]$, $\frac{3}{2}^+[402]$ and $\frac{11}{2}^-[505]$ bands. Table V shows a summary of the present suggestions which differ from the previous ones or are completely new.

### 3.1. *The $N = 95$ isotones*

From the $N = 95$ nuclei we have chosen the experimentally best known isotones $^{163}$Er and $^{161}$Dy for investigation. The three lowest band heads are in both within a 100 keV energy range [31, 32], and thus their correct mutual order (Figs. 2 and 3) cannot be reconstructed easily by any model. However, the adopted reduction of the recoil term [see eq. (4) and Table I] guarantees the right position of the $\frac{5}{2}^+[642]$ band head relative to the low-lying odd-parity states. The experimentally observed increase of the effective moment of inertia for high-spin states of this even-parity band is here produced by the Coriolis interaction alone. Thus higher-order rotational terms are not needed.

Furthermore, the model predictions for the interband and intraband M1 and E2 transition probabilities between the members of the bands considered satisfactorily correspond to the observations. The only clear discrepancy is the E1 transition between the $\frac{5}{2}^+[642]$ and $\frac{5}{2}^-[523]$ band heads (the prediction is about two orders of magnitude too slow). From the two possible candidates $\frac{9}{2}$, $\frac{3}{2}^-[521]$ or $\frac{11}{2}$, $\frac{5}{2}^-[523]$ for the 319 keV level in $^{161}$Dy, the calculated branching ratios pick out the former in agreement with the previous identification by Bennett et al. [33] (see Fig. 3).

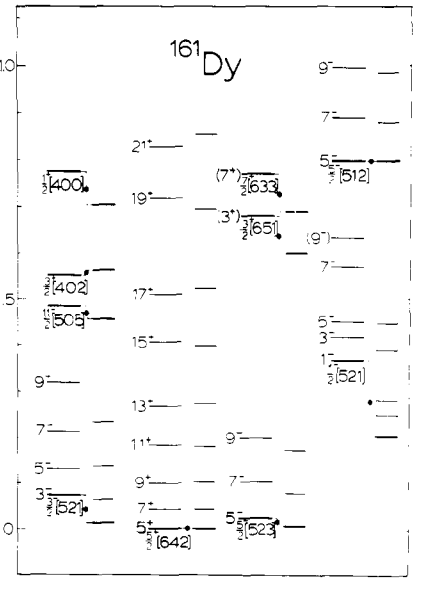


*Fig. 3.* Comparison between the experimental and calculated partial level schemes of $^{161}$Dy.

Table II. *A comparison of the observed and calculated relative intensities of gamma rays from the $\frac{1}{2}^-[521]$ band to the $\frac{5}{2}^-[523]$ and $\frac{5}{2}^-[521]$ bands in $^{161}$Dy and $^{163}$Er (upper and lower numbers, respectively). The experimental intensities have been taken from [35] and [31]. The calculated values correspond to pure M1 or E2 transitions*

| Initial | $\frac{1}{2}, \frac{1}{2}^-[521]$ | | $\frac{3}{2}, \frac{1}{2}^-[521]$ | | $\frac{5}{2}, \frac{1}{2}^-[521]$ | |
|---|---|---|---|---|---|---|
| Final $I, K^\pi[Nn_z\Lambda]$ | $I_{exp}$ | $I_{calc}$ | $I_{exp}$ | $I_{calc}$ | $I_{exp}$ | $I_{calc}$ |
| $\frac{5}{2}, \frac{5}{2}^-[523]$ | 4 | 0.3 | 21 | 3 | 3 | 0.7 |
| | 10 | 0.4 | 3 | 0.5 | 3 | 0.3 |
| $\frac{3}{2}, \frac{3}{2}^-[521]$ | 74 | 74 | 150 | 185 | 7 | 8 |
| | 93 | 93 | 41 | 48 | 6 | 6 |
| $\frac{7}{2}, \frac{5}{2}^-[523]$ | | | 6 | 0.5 | 5 | 0.8 |
| | | | 10 | – | 5 | 0.5 |
| $\frac{5}{2}, \frac{3}{2}^-[521]$ | | | 170 | 170 | 37 | 37 |
| | | | 41 | 41 | 24 | 24 |
| $\frac{7}{2}, \frac{3}{2}^-[521]$ | | | | | 25 | 16 |
| | | | | | 13 | 9 |

The experimental band heads of the $\frac{1}{2}^-[521]$ Nilsson orbital are found as 346 and 367 keV excitations in $^{163}$Er and $^{161}$Dy, respectively. Bunker and Reich [34] have concluded from the direct reaction data and from the calculated Nilsson-model rotational sequency ($a_{the} = 0.88$ [34]) that this band should have a strong $|K-2|$ gamma-vibrational character. The model prediction of its decoupling parameter $a_{ws} = 0.41$, however, is consistent with the experimental value 0.45 as the calculated level spacings of Figs. 2 and 3 immediately show. Moreover, the predicted branching ratios to the members of the $\frac{3}{2}^-[521]$ and $\frac{5}{2}^-[523]$ bands in Table II strongly support an almost pure single-particle nature for the $\frac{1}{2}[521]$ band. According to [33] the direct reaction cross sections fit the expected Nilsson-model pattern for this band in $^{161}$Dy, too.

The experimental value of the decoupling parameter $a = 0.55$ [32] for the suggested $\frac{1}{2}^-[530]$ band in $^{161}$Dy [33] is in serious contradiction with the present prediction $a_{ws} = 0.01$. Thus that identification is very questionable and we have omitted the $\frac{1}{2}^-[530]$ band from Fig. 3. The $\frac{5}{2}^-[512]$ assignment proposed [33] for the 798 keV level has now been confirmed by comparing its decay properties with the calculated ones. The $\frac{7}{2}^-$ and $\frac{9}{2}^-$ members of this band have been previously assigned by Nybø et al. [36]. In $^{163}$Er Tjøm and Elbek [37] have reported the existence of the same band. We, however, propose the $\frac{9}{2}^-$ member to be at 827 keV instead of 805 keV [37] (see Fig. 2).

Unfortunately the experimental information [32] about the two $\frac{3}{2}^+$ states at 550 and 678 keV in $^{161}$Dy is ambiguous, and since the calculated branching ratios do not offer any advice for their identification, we have made the tentative choice displayed in Fig. 3. A spin-parity assignment of $\frac{7}{2}^+$ has been proposed [33] for the 678 keV level, too, but it is ruled out by a comparison with the predicted branching ratios. In $^{161}$Dy [32] we assign the 770 keV level speculatively as the $\frac{7}{2}^+[633]$ band head. A more accurate discussion of these states is given in [33] and references therein. From the corresponding $\frac{3}{2}^+$ levels populated in the decay of $^{163}$Tm [31] we suggest the 619 keV excitation to be $\frac{3}{2}^+[651]$ band head.

### 3.2. *The N = 93 isotones*

Figures 4 and 5 clearly demonstrate the strong increase of mixing in the $\frac{5}{2}^+[642]$ rotational band from $^{157}$Gd to $^{161}$Er. The main contributor to this effect is the growth of the Coriolis interaction by thirty per cent. (cf. the $k$ values in Table I), but also the energy difference between the $\frac{3}{2}^+[651]$ and $\frac{5}{2}^+[642]$ band heads has its effect. The wrong order of the calculated high-spin positive-parity excitations in $^{161}$Er is difficult to reverse without destroying the qualitatively correct coupling obtained for the $\frac{5}{2}^+ - \frac{13}{2}^+$ members of the band.

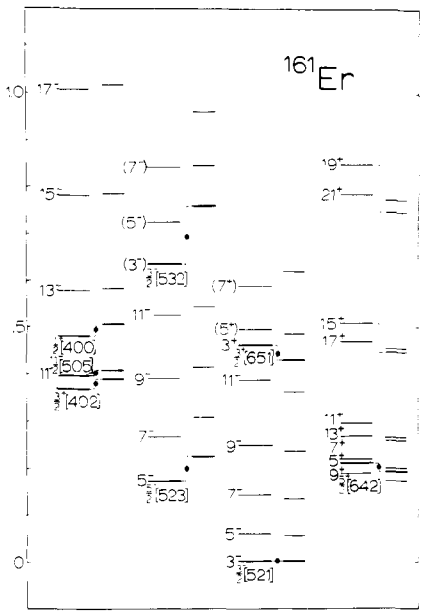


*Fig. 4.* Comparison between the experimental and calculated partial level schemes of $^{161}$Er.

The decay of $^{161}$Tm [38] populates two $\frac{3}{2}^+$ levels at 369 and 463 keV excitations in $^{161}$Er. By comparing the decay properties of these levels with the predictions, we can conclude that the wave function of the lower state includes at most ten per cent of a $\frac{3}{2}^+[651]$ admixture. Thus it is justifiable to make the $\frac{3}{2}^+[402]$ and $\frac{3}{2}^+[651]$ assignments to these levels (see Fig. 4). The tentative $\frac{5}{2}^+$ and $\frac{7}{2}^+$ spins and parities have been proposed [38] for the levels at 496 and 590 keV, respectively. We designate these states from the relative gamma intensities as the first and second rotational members of the $\frac{3}{2}^+[651]$ band.

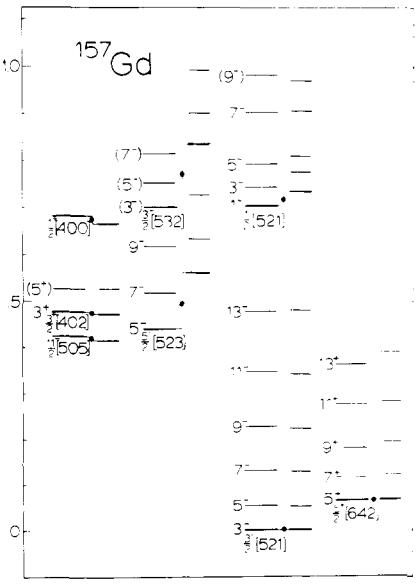


*Fig. 5.* Comparison between the experimental and calculated partial level schemes of $^{157}$Gd.

Figure 4 shows three tentative members of the $\frac{3}{2}^-[532]$ band. Two of these, namely the 725 and 843 keV odd-parity levels, have been suggested previously [38] to have spins of $\frac{3}{2}$ and $\frac{5}{2}$, respectively. However, consideration of the predicted gamma intensities, especially for transitions to the members of the ground band, allows only the spins $\frac{5}{2}$ and $\frac{7}{2}$. We have assigned the 635 keV level populated in the $(d, t)$ reaction [37] as the head of this $\frac{3}{2}^-[532]$ band. The level spacings support the present identification, too.

In $^{157}$Gd the overall energy fit (Fig. 5) is satisfactory, and the calculated branching ratios confirm the previous assignments [39] for the levels below 430 keV. The predicted M1 transition rates from the members of the $\frac{5}{2}^-[523]$ rotational band to the ground band are too fast, however. To explain the decay properties of the $\frac{3}{2}^+$ level at 477 keV, we need a small admixture of the $\frac{3}{2}^+[402]$ and $\frac{3}{2}^+[651]$ orbitals in its final wave function. In addition, the single-particle energies of these states have to be sufficiently close to each other to cause the necessary mixing. This situation was reached with the present model, however, only with a deformation ten per cent larger than the systematics of Table I would indicate. The classification of the levels above 500 keV excitation still remains tentative because of the poor knowledge of their decay properties. Thus all the assignments given here for $^{157}$Gd agree with the previous ones [39].

### 3.3. *The $N = 91$ isotones*

The structure of the $N = 91$ nuclei is characterized by the systematically varying strength of the Coriolis force (see Fig. 1), which is displayed most clearly in the change of the mutual order of the low-spin states in the perturbed $\frac{3}{2}^+[651]$ rotational band. Another important feature is the position of the $\frac{3}{2}^-[521]$ state as compared with the even-parity band. The variation of the deformation parameter $\eta_4$ (cf. Table I) and the recoil term (4) give here the required effect.

Ignoring for the moment the well-established low-lying states of $^{157}$Dy [39] seen in Fig. 6, one has to consider the interesting levels in the 300–600 keV energy region. Of those the $\frac{5}{2}^-$ and $\frac{7}{2}^-$ states at 341 and 420 keV belong to a previously assigned $\frac{5}{2}^-[523]$ Nilsson band [36, 39]. The wave functions of both these states expressed explicitly in [36] are strongly Coriolis-mixed with the nearby $\frac{3}{2}^-[532]$ orbital. In our calculation the situation is the same, although the latter band head is now located at 399 keV instead of 350 keV [36]. This interpretation agrees with that of [39]. However, the $\frac{5}{2}, \frac{3}{2}[532]$ assignment is now suggested for the 508 keV level (cf. Table V).

We can confirm the above $\frac{5}{2}^-[523]$ and $\frac{7}{2}, \frac{5}{2}^-[523]$ assignments with the predicted gamma branching ratios, which also require the existence of a strong 258.1 keV E1 transition from the 420 keV level to the $\frac{9}{2}^+$ state at 162 keV. This relocation is supported also by its weakened lower coincidences with the 86.5 and 147.7 keV gamma rays [41] ($T_{1/2}(\frac{9}{2}^-) = 1.3\,\mu$s). As the very tentative level at 406 keV [41] is mainly built on the 258.1 keV transition, we omit it from the level scheme. We follow the same policy for the 274 keV level [41] and place the corresponding transition to de-excite the 508 keV level. The $\frac{9}{2}^-$ member of the $\frac{5}{2}^-[523]$ band has been proposed to exist at 519 keV [36]. However, the observed transitions from the 527 keV level populated in the decay of $^{157}$Ho [42] are not consistent with the tentative $\frac{7}{2}^-$ assignment [39], but agree with the model predictions for the $\frac{9}{2}, \frac{5}{2}^-[523]$ state. This tentative interpretation is supported by the observed $(\tau, \alpha)$ cross-section in the reaction study of Grotdal et al. [43].

Moreover, we make the proposals $\frac{5}{2}, \frac{1}{2}^-[530]$ and $\frac{7}{2}, \frac{1}{2}^-[530]$ for the 897 and 990 keV levels, respectively. Accordingly we are able to locate an intensive, previously unplaced, 828.1 keV transition to connect the $(7/2^-)$ 990 keV state to the $\frac{9}{2}^+$ state at 162 keV. Thus we have confirmed three previously ambiguous assignments and proposed four new ones for the odd-parity states discussed.

The even-parity states established in $^{157}$Dy are predominantly members of the strongly perturbed $\frac{3}{2}^+[651]$ Nilsson band. The calculated level spacings displayed in the right-hand column of Fig. 6 are in satisfactory agreement with observations, if one takes into account the number of parameters used ($A$ and $k$). The experimental information on the other even-parity states is unfortunately so scarce that it does not offer a posssibility for any reasonable comparison.

In $^{155}$Gd the unperturbed energies of the $\frac{3}{2}^-[532]$ and $\frac{5}{2}^-[523]$ states are again close enough to cause a considerable mixing. According to our interpretation the order of these orbitals has been interchanged as compared to $^{157}$Dy (cf. Figs. 6 and 7). The 287 keV level has been assigned as a $\frac{3}{2}^-[532]$ band head previously by Meyer et al. [44] in agreement with our identification, but in contradition with the level scheme of Kroger and Reich [45], from which we have also omitted a $\frac{3}{2}^+$ state at 235 keV. The reason is that our calculation con-

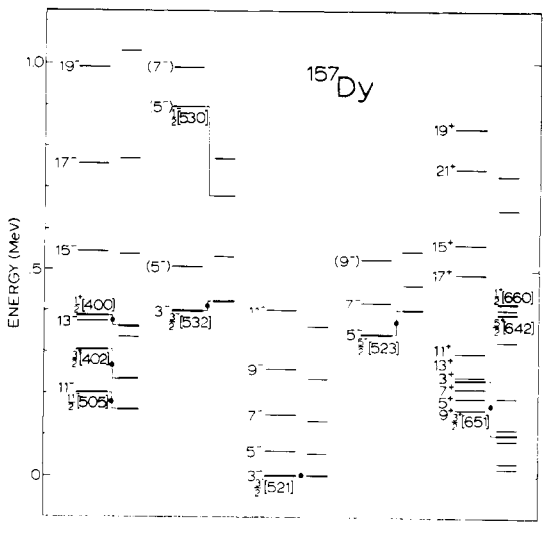


*Fig. 6.* Comparison between the experimental and calculated partial level schemes of $^{157}$Dy.

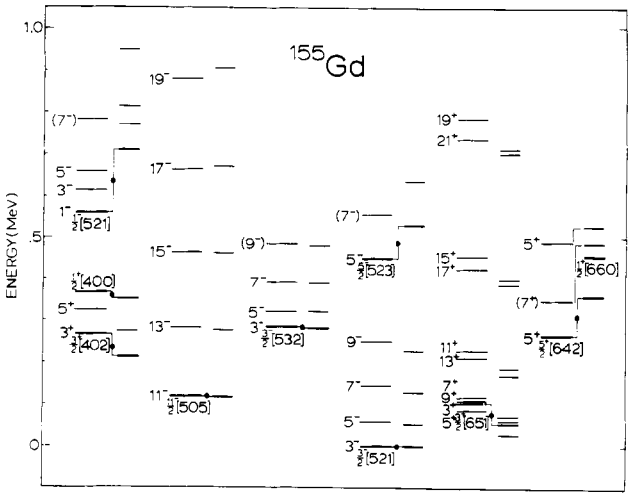


*Fig. 7.* Comparison between the experimental and calculated partial level schemes of $^{155}$Gd.

firms the placement of the 216.0 keV transition to de-excite the new $\frac{5}{2}^-$ level at 321 keV [44]. The replacements of the other intensive transitions which fed or de-excited this spurious $\frac{3}{2}^+$ level are also pointed out in [44] in agreement with the present predictions.

Two of those transitions depopulate the same 321 keV level which has the previous $\frac{5}{2}^-[523]$ assignment [45, 46]. However, its decay especially to the ground band favours the present $\frac{5}{2}$, $\frac{3}{2}^-[532]$ assignment. The levels at 393 and 485 keV are populated in $(d, t)$ reactions [46, 47], and we identify them tentatively as members of the $\frac{3}{2}^-[532]$ band instead of $\frac{5}{2}^-[523]$ (see Table V).

The existence of the 346 keV level [44] is based only on one ground-state transition, and as this gamma ray can be placed also to de-excite the 451 keV level (the experimental $\alpha_K$ allows E2 or alternatively E1 multipolarity), we omit the 346 keV level from Fig. 7. The 451 keV state has been previously proposed to be the $\frac{5}{2}^-[512]$ band head [44], but on the basis of deduced systematics we designate it as the $\frac{5}{2}^-[523]$ band head and the 556 keV state as the $\frac{7}{2}^-$ member of the band.

The well-established $\frac{1}{2}^-[521]$ rotational band is reproduced nicely by a calculation with the predicted decoupling parameter $a_{ws} = 0.39$. The agreement between the observed and calculated branching ratios from the $\frac{1}{2}$, $\frac{3}{2}$ and $\frac{5}{2}$ members of this band is again amazing, without any vibrational admixtures proposed [44].

In $^{155}$Gd the predicted coupling between the even-parity states emanating from the $i_{13/2}$ shell is weaker than in $^{157}$Dy, as the level spacings of the $\frac{3}{2}^+[651]$ band show. The low-spin members are reproduced satisfactorily, however. The right-hand column of Fig. 7 shows some other low-spin states which are identified as members of the $\frac{5}{2}^+[642]$ or $\frac{1}{2}^+[660]$ band. From those states we have confirmed the tentative $\frac{7}{2}$, $\frac{5}{2}^+[642]$ proposal [44] for the level at 350 keV. The well-known $\frac{5}{2}^+$ state at 489 keV has been classified previously as a $\frac{5}{2},\frac{1}{2}^+[400]$ rotational state [44]. The level decays, however, predominantly to the members of the $\frac{3}{2}^+[651]$ and $\frac{5}{2}^+[642]$ bands (especially via the 138.3 keV transition to the $\frac{7}{2}$, $\frac{5}{2}^+[642]$ state) and no transition to the $\frac{3}{2}^+[402]$ band head has been observed [45]. These facts together with a very nice agreement with predicted branching ratios justify the present $\frac{5}{2},\frac{1}{2}^+[660]$ assignment. According to the calculation the only realistic candidate for the experimental 427 keV level is the $\frac{1}{2}^+[660]$ band head. However, the spin value of $\frac{1}{2}$ does not allow the existence of

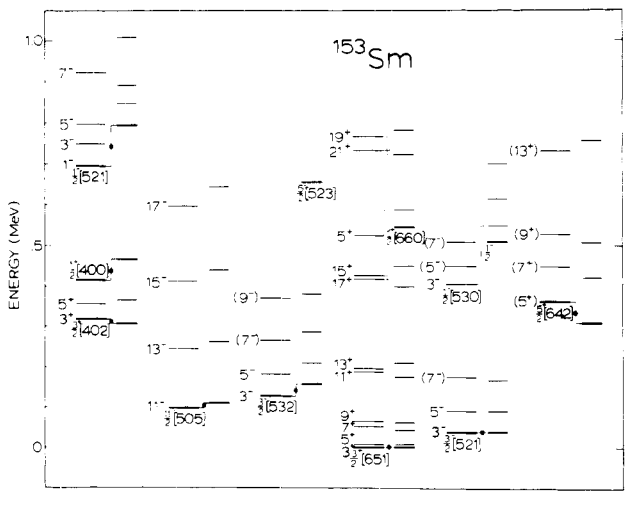


*Fig. 8.* Comparison between the experimental and calculated partial level schemes of $^{153}$Sm.

the depopulating 367.4 keV E1 transition to the $\frac{5}{2}^-$ member of the ground band [45].

The characteristic Coriolis-intermixed even-parity band, which builds again on the $\frac{3}{2}^+[651]$ Nilsson orbital, exists in $^{153}$Sm as the ground band. Figure 8 shows that the calculated high-spin members of this band are here even in a wrong order as compared with the experimental results [48]. In spite of that we would like to emphasize that the model predicts the relative branchings of intraband transitions as the observations presuppose [48]. The same Coriolis interaction produces also a perturbed structure for the $\frac{5}{2}^+[642]$ side band, as the right-hand column of Fig. 8 shows. For every calculated level of this highly tentative band we can identify a corresponding state in the experimental level scheme [48, 49]. These two-by-two connections are based on the predicted and observed transitions from each individual level. For the same reason, combined with the deduced systematics in the other $N = 91$ nuclei we designate the 524 keV level as a $\frac{5}{2}$, $\frac{1}{2}^+[660]$ rotational state.

Among the low-lying excitations are two $\frac{3}{2}^-$ states of which we cannot assure unambiguously which one should be the $\frac{3}{2}^-[521]$ or $\frac{3}{2}^-[532]$ band head. As the level spacings within both these bands are also strikingly the same, we have tentatively adopted the previous classification [49]. The assignment of the other odd-parity bands shown in Fig. 8 are based predominantly on the direction reaction data [47] and partly on the decay properties of various states. Unfortunately the predicted branching ratios do not offer any useful probe for reliable conclusions.

In the $^{152}$Sm$(n, \gamma)^{153}$Sm reaction study [50] the existence of many low-lying even-parity levels has been proposed. Because of their uncertainty we have, however, dropped some of them. Moreover, a comparison with the other $N = 91$ nuclei does not support the existence of such excitations.

The calculated energies of the $\frac{7}{2}^+[404]$ and $\frac{11}{2}$, $\frac{9}{2}^-[514]$ states are, if one applies the shifts presented in the seventh and eight column of Table I, in all three nuclei considered within 100 keV of their experimental values [43, 45, 47].

The results of our calculation concerning $^{151}$Nd, which has a similar structure to $^{153}$Sm, will be presented in detail with some new experimental results from the $^{150}$Nd$(d, p\gamma)$ $^{151}$Nd measurements [51].

### 3.4. *The N = 89 isotones*

The $N = 89$ nuclei are usually considered as transitional or as nuclei in the region of rapidly changing deformation. However, recent experimental information on the low-spin states indicates the existence of a well-defined deformation in these nuclei.

The high-spin ($I \geqslant \frac{9}{2}$) members of the even-parity band with $I + \frac{1}{2}$ odd are experimentally well established and also qualitatively described with various versions of the particle-rotor model [5, 7, 11, 16]. This band is built on the $\frac{1}{2}^+[660]$ Nilssson orbital and has such a regular decoupled structure that our calculation reproduces its level spacings (see Figs. 9–11) by varying the attenuation factor $k$ as a function of the proton number, as Fig. 1 shows. Hjorth and Klamra [16] have recently considered with critisism the validity of these phenomenological Hamiltonians – even at low angular velocities – particularly in describing the rotational excitations of the $i_{13/2}$ system. The generally poor knowledge of its low-spin members is clearly demonstrated in the recent compilation of these $\frac{1}{2}^+$, $\frac{3}{2}^+$, $\frac{5}{2}^+$ and $\frac{7}{2}^+$ states in the $N = 89$ nuclei by Pinston et al. [11]. We want to emphasize the importance of knowing the positions of the low-

spin band heads for calculations of this kind (see the fourth paragraph of Subsection 2.2).

Another common feature in the spectra of the $N = 89$ nuclei is the existence of the $\frac{11}{2}^-[505]$ rotational band, for which the effective intertial parameter is smaller than for other bands in the same nucleus. The present model accounts for this effect almost entirely through the Coriolis coupling between the $h_{11/2}$ orbitals. We have shifted the interaction orbitals by the same amount towards the Fermi level (cf. Table I). The method is supported by the approximately correct excitation energies predicted for the known $\frac{11}{2}^-$, $\frac{9}{2}^-[514]$ states (not shown in the figures).

In addition, we are forced to reduce the calculated single-particle energies of the $\frac{1}{2}^-[530]$ state to reach the correct coupling with the $\frac{3}{2}^-[521]$ state. The necessary shifts are 600, 400 and 500 keV for $^{155}$Dy, $^{153}$Gd and $^{151}$Sm, respectively. Since the experimental energies of the other low-spin odd-parity states indicate a mixing of the $f_{7/2}$ orbitals, we have had to shift also the $\frac{3}{2}^-[532]$ single-particle state by 500 and 200 keV away from the Fermi level in $^{155}$Dy and in $^{153}$Gd, respectively. As all these shifts take place near the Fermi surface they affect the BCS calculation and thus also the resulting wave functions of all the low-lying states. In our opinion the final wave functions are, however, more realistic than they would be without the shifts, as indicated by more correct coupling phenomena among the relevant odd-parity states. This conclusion is supported by the nice agreement between the predicted and observed energy level systematics shown in Figs. 9–11.

The ground-state band of $^{155}$Dy has been suggested previously to be built on the $\frac{3}{2}^-[521]$ Nilsson orbital [1, 2], but recently Hjorth and Klamra [16] have proposed as another possibility $\frac{3}{2}^-[532]$. The latter interpretation has been deduced from the strongly perturbed structure of that ground band when it is extended up to the spin member $\frac{15}{2}^-$. In our calculation, however, this phenomenon is reproduced (see Fig. 9) purely as a result of the Coriolis coupling between the $\frac{3}{2}^-[521]$ and $\frac{1}{2}^-[530]$ orbitals with the predicted decoupling parameter $a_{ws} = 2.1$. The previous calculation [2] has performed with the value $a = -2.5$ despite the Nilsson-model prediction $a = 1.2$. The intraband branching ratios also for the high-spin members of the band support the $\frac{3}{2}^-[521]$ choice.

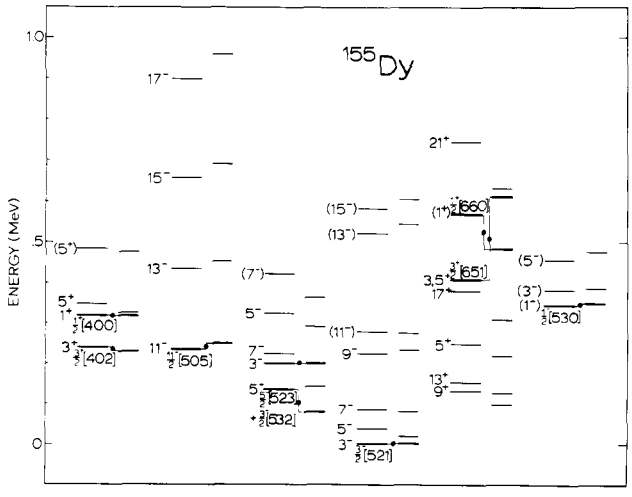


*Fig. 9.* Comparison between the experimental and calculated partial level schemes of $^{155}$Dy. For the levels of the $\frac{3}{2}^+[651]$ side band see the discussion in the text. The amplitudes of the $\frac{1}{2}^-[541]$ and $\frac{3}{2}^-[532]$ orbitals are remarkable in the wave functions of the $\frac{3}{2}$, $\frac{1}{2}^-[530]$ and $\frac{5}{2}$, $\frac{1}{2}^-[530]$ states and thus the band does not resemble the decoupled structure, although $a_{ws} = 2.1$.

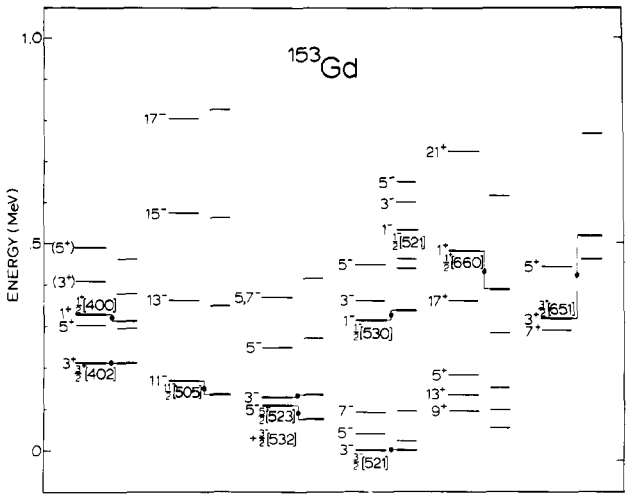


*Fig. 10.* Comparison between the experimental and calculated partial level schemes of $^{153}$Gd.

In Fig. 9 the other low-lying odd-parity levels, grouped into the third column, are built on the strongly Coriolis-intermixed $\frac{3}{2}^-$ and $\frac{5}{2}^-$ orbitals emanating from the $f_{7/2}$ shell. The $\frac{5}{2}^-$ state at 136 keV and the $\frac{3}{2}^-$ state at 202 keV are proposed as heads of the $\frac{5}{2}^-[523]$ and $\frac{3}{2}^-[532]$ bands [1, 2]. The predicted gamma branching ratios support the previous tentative assignments, with the important exception that an intensive 115.5 keV E2 transition from the 202 keV level [1] will be placed between the even-parity excitations (cf. further text). For the $\frac{7}{2}^-$ and $\frac{5}{2}^-$ levels at 224 and 325 keV our calculation supports the previous identifications [1, 2] (see Fig. 9). By its decay properties we have tentatively classified the uncertain level at 423 keV [45] to correspond to the $\frac{7}{2},\frac{3}{2}^-[532]$ state, although the previous candidate for this assignment [1] is the level at 483 keV.

On the basis of the present knowledge we will propose some rearrangements in the previous level scheme of $^{155}$Dy [1, 45]. First, we are convinced that, in distinction to the previous placement of the 115.5 keV gamma ray, the $\frac{5}{2}^+$ level at 248 keV decays via this E2 transition to the isomeric $\frac{9}{2}^+$ state at 132 keV [52]. This is also supported by the lack of any upper coincidences with the 115.5 keV transition in [45]. Second, the uncertain placement [1] of the strong 219.0 keV M1 transition

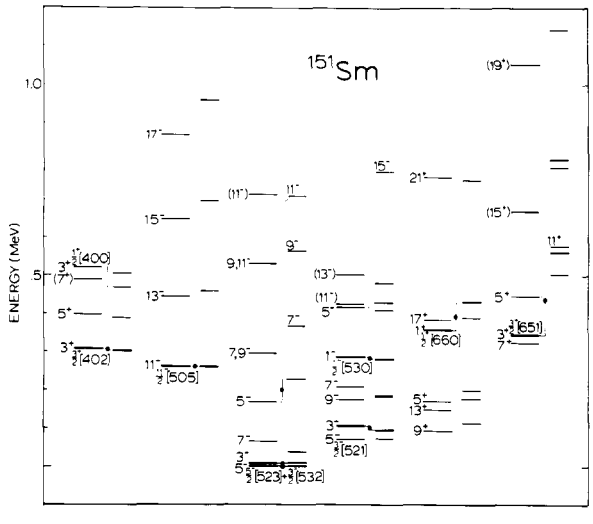


*Fig. 11.* Comparison between the experimental and calculated partial level schemes of $^{151}$Sm.

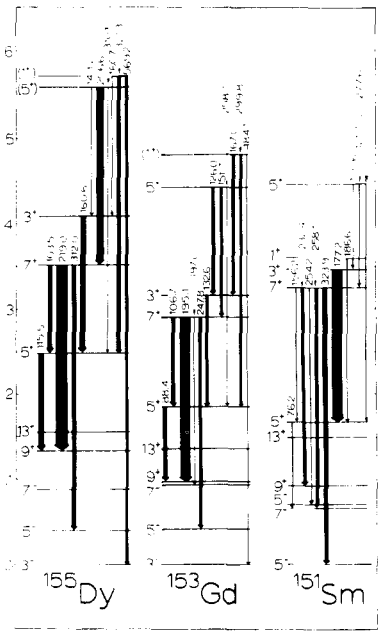


*Fig. 12.* Systematics of the $\frac{3}{2}^+[651]$; $\frac{7}{2}$, $\frac{3}{2}^+[651]$ and of the tentative $\frac{5}{2}$, $\frac{3}{2}^+[651]$ levels in the $N = 89$ nuclei (energy scale in MeV). The spin of each level is given in units of $\hbar/2$. The intensity of the strongest transition is normalized to be the same for all nuclei presented. The widths of the other lines represent the relative intensities of gamma rays [1, 3, 6]. In $^{155}$Dy the transitions from the $\frac{5}{2}^+$, $\frac{7}{2}^+$ and $(\frac{5}{2}^+)$ levels are placed according to the results of the present calculation. The corresponding rearrangements in $^{153}$Gd have been made for gamma rays depopulating the $\frac{7}{2}^+$ level and for the 151.7 and 299.8 keV transitions. The assignments of the levels are given in Figs. 9–11 and the explicit wave functions of the $\frac{9}{2}^+$ and $\frac{7}{2}^-$ states in [52].

should be changed: according to our interpretation this transition de-excites, together with the 312.0 keV E1 transition, a new level at 351.4 keV as Fig. 12 shows. Thus these two gamma rays populate the isomeric $\frac{9}{2}^+$ state and the $\frac{5}{2}^-$ member of the ground band, respectively. The existence of the level in question is well established by the observed but not previously understood coincidence relationship [1] between an unplaced 206.6 keV gamma ray and the transitions mentioned. The multipolarities of these transitions fix, with the systematics deduced in the $N = 89$ nuclei (Fig. 12), the spin and parity of the 351.4 keV level as $\frac{7}{2}^+$. By these arguments we designate the 351 level as $\frac{7}{2},\frac{3}{2}^+[651]$ state (cf. the corresponding levels of Figs. 10 and 11).

As the most probable multipolarity of the 206.6 keV transition is E2, the parity of the new 558.0 keV level should be positive. Direct reactions [2] populate also a level at 555 keV with a probable angular momentum transfer of 2 or 3 units. As a conclusion we make a speculative $\frac{5}{2}$, $\frac{3}{2}^+[651]$ assignment for the 558 keV level.

One interesting even-parity state exists at 409 keV with spin $\frac{1}{2}$, $\frac{3}{2}$ or $\frac{5}{2}$ [45]. By comparing the relative intensities of the observed gamma rays with the model predictions in Table III we conclude that this level could be the $\frac{3}{2}^+[651]$ band head (Fig. 9), although this assignment has been previously suggested for the 655 keV level [2]. The same arguments favour a tentative $\frac{1}{2}^+[660]$ identification for the 659 keV level instead of the $\frac{3}{2}^+$ proposal [1, 16]. The 484 keV level has been proposed to be an odd-parity state [1] or alternatively a $\frac{5}{2},\frac{1}{2}^+[400]$ rotational state [2]. The latter assignment agrees with the present one, which is based mainly on the existence of a 243.7 keV transition to the $\frac{3}{2}^+[402]$ band head, and thus follows the observed systematics in other $N = 89$ nuclei.

Table III. *A comparison of the experimental [1] and predicted relative intensities of gamma rays depopulating the $\frac{3}{2}^+[651]$ band head at 408.5 keV in $^{155}$Dy (cf. Fig. 12). The calculated values correspond to pure E1 or M1 transitions*

| Transition energy (keV) | Final state $I, K^\pi[Nn_z\Lambda]$ | Relative $I_\gamma$ | |
|---|---|---|---|
| | | exp. | calc. |
| 408.5 | $\frac{3}{2}, \frac{3}{2}^-[521]$ | 11.0 | 11.0 |
| 369.3 | $\frac{5}{2}, \frac{3}{2}^-[521]$ | –[a] | 0.1 |
| 272.2 | $\frac{5}{2}, \frac{5}{2}^-[523]$ | 4.7 | 0.8 |
| 206.1 | $\frac{3}{2}, \frac{3}{2}^-[532]$ | –[b] | 0.1 |
| 160.6 | $\frac{5}{2}, \frac{1}{2}^+[660]$ | 10.0 | 12.0 |

[a] A less probable placement.
[b] Observed only in coincidence spectra.

In the column farthest to the right in Fig. 9 we give a highly tentative proposal for the three lowest members of the $\frac{1}{2}^-[530]$ band. Of these, the 456 keV state has been suggested to have a vibrational character [1], but its decay properties nicely correspond to our predictions for the $\frac{5}{2}$, $\frac{1}{2}^-[530]$ state. In fact, it has been used as a reference level in making the necessary 600 keV shift of the $\frac{1}{2}^-[530]$ band head.

Outside Fig. 9 we can state that the calculation supports the previous $\frac{5}{2}^-[512]$ suggestion [1] for the 557 keV level, but disagrees with the $\frac{7}{2},\frac{5}{2}^-[512]$ proposal for the 703 keV level (see Table V).

In $^{153}$Gd the ground band, known up to the $\frac{7}{2}$ member only, has been usually assigned as a $\frac{3}{2}^-[521]$ band [3, 5, 49], but recently Guttormsen et al. [17] have proposed the $\frac{3}{2}^-[532]$ Nilsson assignment by comparison with $^{151}$Sm. We discuss that possibility in more detail a little later. Obviously the ground-band states are not pure but are mixed with the $\frac{1}{2}^-[530]$ orbital as reported by Løvhøiden et al. [5]. In our calculation, however, this coupling is too strong even though we have shifted the $\frac{1}{2}^-[530]$ state to its experimental energy.

The odd-parity states at 110 and 129 keV again come from the admixture of the $\frac{3}{2}^-$ and $\frac{5}{2}^-$ orbitals originating from the $f_{7/2}$ shell. As a result, all the levels drawn in the third column of Fig. 10 have complex wave functions resembling those explicitly expressed by Tuurnala [13]. The parity of the 250 keV level has been deduced to be negative [3, 53], although the angular distribution [5] observed in the $(d, t)$ reaction favours an $l = 2$ transfer. We tentatively assign this level as a $\frac{5}{2}$, $\frac{3}{2}^-[532]$ state and correspondingly the 369 keV level as a $\frac{7}{2}^-$ rotational member of the same band (see Fig. 10).

The calculated level spacings of the $\frac{1}{2}^-[530]$ band are here not as good as in $^{155}$Dy if the previous identification [49], which is based mainly on direct reaction data, is correct. A serious contradiction, however, exists between the experimental decoupling parameter $a = -0.55$ [49] and the values $a = 1.4$ [13] or $a_{ws} = 1.8$.

We have not discussed before the proposed $\frac{1}{2}^-$ state at 195 keV [3] because it will be omitted from the level scheme of $^{153}$Gd. Instead, we propose the existence of a new level at 290.2 keV. This level decays to the ground band via E1 transitions and via a 195.1 keV M1 transition to the isomeric $\frac{9}{2}^+$ state at 95 keV, as Fig. 12 shows. The lack of any observed lower coincidences [3] with the 195.1 keV gamma ray is explained by the 3.5 μs half-life of the $\frac{9}{2}^+$ state [52]. As a consequence of this new interpretation, also some other transitions have to be replaced and the 346 keV level be omitted from the previous level

Table IV. *A comparison of the experimental newly placed [3] and predicted relative intensities of gamma rays depopulating the $\frac{7}{2}, \frac{3}{2}^+[651]$ state at 290.2 keV in $^{153}$Gd (cf. Fig. 12). The calculated values correspond to pure E1 or M1 transitions.*

| Transition energy (keV) | Final state $I, K^\pi[Nn_z\Lambda]$ | Relative $I_\gamma$ | |
|---|---|---|---|
| | | exp. | calc. |
| 248.7 | $\frac{5}{2}, \frac{3}{2}^-[521]$ | 5.0 | 1.0 |
| 197.0 | $\frac{7}{2}, \frac{3}{2}^-[521]$ | 2.3 | 0.5 |
| 195.1 | $\frac{9}{2}, \frac{1}{2}^+[660]$ | 27.0 | 27.0 |
| 180.4 | $\frac{5}{2}, \frac{5}{2}^-[523]$ | – | – |
| 106.7 | $\frac{5}{2}, \frac{1}{2}^+[660]$ | 8.0 | 7.2 |

scheme [3]. It is worth noting that this rearrangement is in full agreement with the observed $\gamma$–$\gamma$ and $e$–$\gamma$ coincidences [54]. The spin and parity of the 290 keV level are deduced to be $\frac{7}{2}^+$. By comparing the branching ratios of the newly placed and predicted gamma rays in Table IV, we can deduce the $\frac{7}{2}, \frac{3}{2}^+[651]$ assignment for this level (see Fig. 10).

The decay of $^{153}$Tb [3, 53] populates a $\frac{3}{2}^+$ state at 316 keV for which we have not found any previous explanation with the Nilsson model. From the predicted branching ratios and deduced systematics (cf. Table III and Fig. 12) we conclude that this level is the head of a perturbed rotational band built on the $\frac{3}{2}^+[651]$ state. This assignment has been suggested previously [5] for the 504 keV level populated by $l = 2$ transfer in the direct reactions. The third level in the right-hand column of Fig. 10 is the $\frac{5}{2}^+$ state at 442 keV which has been tentatively identified as the $\frac{5}{2}, \frac{1}{2}^+[400]$ state [5]. However, it decays only to the even-parity states belonging to the Coriolis-intermixed $N = 6$ bands according to the present interpretation. This fact supports our speculative $\frac{5}{2}, \frac{3}{2}^+[651]$ assignment. As the calculated energy of the $\frac{11}{2}^+$ member of this side band is about 100 keV higher than the energy of the $\frac{7}{2}^+$ state, the very tentative placement of the $\frac{11}{2}^+$ state at 221 keV [49, 55] may be wrong (cf. Fig. 11). Moreover, we can confirm the previous $\frac{1}{2}^+[660]$ proposal [5] for the 484 keV level. The tentative assignment $\frac{5}{2}, \frac{1}{2}^+[400]$ which we propose for the 490 keV level is based on the observed transition to the $\frac{3}{2}^+[402]$ band head at 212 keV (cf. Table V).

Figure 12 shows, among other things, a compilation of the decay properties of the $\frac{7}{2}^+$ states in the $N = 89$ nuclei considered. If one accepts the present identifications, the proposed $\frac{3}{2}^-[532]$ assignment for the ground state of $^{153}$Gd [17] seems to be wrong, as the relative intensities of the transitions from the $\frac{7}{2}^+$ states in $^{153}$Gd and in $^{151}$Sm very clearly show.

The lack of any clear rotational band structure in the low-lying odd-parity excitations of $^{151}$Sm has caused difficulties in efforts to describe the observed states with particle-rotor models [7–9]. A recent calculation performed with an extended Nilsson model by Guttormsen et al. [17] is a promising attempt to understand this structure. The present result is displayed in Fig. 11, where the levels originating from the same shell-model state have been grouped to the same column.

The lowest $\frac{3}{2}^-$ excitation at 5 keV seems to be an almost pure $\frac{3}{2}^-[532]$ band head, while the wave functions of the ground state and the third $\frac{5}{2}^-$ state at 168 keV are strongly admixed, each one containing about the same amount of the $\frac{3}{2}^-[532]$ and $\frac{5}{2}^-[523]$ orbitals. Anyway, we assign the 168 keV state as the $\frac{5}{2}^-[523]$ band head. In the earlier calculation [17] this strong mixture was not achieved and the 168 keV level was not grouped among the levels classified as an $f_{7/2}$ band. Figure 11 shows that we associate with the same coupling the $\frac{7}{2}^-$ state 66 keV, as well as the experimental $\frac{7}{2}^-$, $\frac{9}{2}^-$ and $\frac{9}{2}^-$, $\frac{11}{2}^-$ states at 295 and 530 keV, respectively. The explicit wave functions of the $\frac{7}{2}^-$ state are given in [17, 52]. The 530 keV level was assigned in [17] as a practically pure $\frac{13}{2}^-$ member of the $h_{9/2}$ band, but the Coulomb excitation data [56, 57] agree rather well with the present identification. We have also identified the 715 keV excitation [56] as the calculated $\frac{11}{2}^-$ rotational state at 706 keV.

In general, the present assignments for the low-spin odd-parity states agree with [17] and thus completely differ from the earlier proposals [8, 57]. The fourth column of Fig. 11 shows our suggestion for the states generated mainly by the Coriolis coupling of the $\frac{1}{2}^-[530]$ and $\frac{3}{2}^-[521]$ orbitals. The oscillator potential prediction for the decoupling parameter of the $\frac{1}{2}^-[530]$ state ($a = 0.89$ [17]) differs by a factor of two from our value $a_{ws} = 2.0$, giving rise to some differences with the calculated level spacings. In addition, we have included in the calculation the $\frac{5}{2}^-[512]$ state, which also has appreciable amplitudes in the wave functions of the states in question. Since the published experimental information [9] is not adequate for an unambiguous interpretation of the high-spin states belonging to this band, we identify its $\frac{11}{2}^-$, $\frac{13}{2}^-$ and $\frac{15}{2}^-$ members differently from [17]. For the calculated $\frac{15}{2}^-$ state (Fig. 11) we have no experimental counterpart, however,. The $\frac{5}{2}^-$ level observed in the decay study of [6] we designate as the $\frac{5}{2}, \frac{1}{2}^-[530]$ state from the predicted branching ratios.

For the remaining odd-parity states observed below 500 keV [57] the calculation predicts a $\frac{1}{2}^-[541]$ origin. Those poorly known excitations are not included in Fig. 11 or in our further discussion.

In the previous description of the even-parity states in $^{151}$Sm [9] some low-spin excitations were left without any reliable assignment. According to [11] there exists some ambiguities even in classifying the close-lying $\frac{3}{2}^+[402]$ and $\frac{3}{2}^+[651]$ band heads. However, a comparison between the predicted and observed branching ratios of the 307 and 345 keV levels points out rather clearly that the former should be the $\frac{3}{2}^+[402]$ band head. Likewise the 396 keV level is probably its first and the $\frac{7}{2}$ state at 490 keV possibly its second rotational state. This assignment of the 490 keV state (see Fig. 11) is supported by the observed log ft values [6]. We can also confirm the proposed $\frac{3}{2}, \frac{1}{2}^+[400]$ assignment [9] of the 521 keV level.

Based on the systematics and on the observed transitions from the 324 and 345 keV levels [6] (see Fig. 12), we assign these states as $\frac{7}{2}, \frac{3}{2}^+[651]$ and $\frac{3}{2}^+[651]$, respectively, in agreement with the previous preliminary interpretation [9]. Instead, the speculative $\frac{5}{2}^+[642]$ identification [9] of the 446 keV level is in contradiction with our $\frac{5}{2}, \frac{3}{2}^+[651]$ suggestion (see Fig. 11). The present wave functions of all these states differ clearly from those of [9] since the $\frac{5}{2}^+[642]$ band head is predicted at a considerably higher energy than about 450 keV. The reasonable agreement with the experimentally known high-spin $\frac{15}{2}^+$ and $\frac{19}{2}^+$ members of this $\frac{3}{2}^+[651]$ side band (see Fig. 11) should be taken as additional evidence for the systematics displayed in Fig. 12. Even the experimental absence of the predicted $\frac{11}{2}^+$ member can be explained by the energetically favoured M1 transitions from the $\frac{15}{2}^+$ state to the $\frac{13}{2}^+$ and $\frac{17}{2}^+$ members of the decoupled $\frac{1}{2}^+[660]$ band.

For the higher-lying even-parity states [57] we are not able to make any tentative identifications, though the model predicts the existence of some low-spin states roughly at their experimental energies.

Table V. *A compilation of the previous and present assignments in the N = 95–89 nuclei considered. The references for the previous ones are given in the text. Of two different energy values separated with a semicolon, the former corresponds to the previous and the latter to the present assignment. Two or three energy values separated with commas correspond to the consecutive members of the bands indicated*

| Nucleus | Level energy (keV) | Previous assignment $I, K^\pi[Nn_z\Lambda]$ | Present assignment $I, K^\pi[Nn_z\Lambda]$ |
|---|---|---|---|
| $^{163}$Er | 619 | $\frac{3}{2}^+$ | $\frac{3}{2}^+[651]$ |
| | 805; 827 | $\frac{9}{2}, \frac{5}{2}^-[512]$ | $\frac{9}{2}, \frac{5}{2}^-[512]$ |
| $^{161}$Dy | 319 | $\frac{9}{2}, \frac{3}{2}^-[521]$ | $\frac{9}{2}, \frac{3}{2}^-[521]$ |
| | 798 | $\frac{5}{2}^-[512]$ | $\frac{5}{2}^-[512]$ |
| | | $\frac{1}{2}^-[530]$ band | – |
| | 678 | $\frac{3}{2}^+$ or $\frac{7}{2}^+$ | $\frac{3}{2}^+$ |
| | 770 | – | $\frac{7}{2}^+[633]$ |
| $^{161}$Er | 369 | $\frac{3}{2}^+$ | $\frac{3}{2}^+[402]$ |
| | 463, 496, 590 | $\frac{3}{2}^+, \frac{5}{2}^+, \frac{7}{2}^+$ | $\frac{3}{2}^+[651]$ band |
| | 635, 725, 843 | $-, \frac{3}{2}^-, \frac{5}{2}^-$ | $\frac{3}{2}^-[532]$ band |
| $^{157}$Dy | 399 | $\frac{3}{2}^-[532]$ | $\frac{3}{2}^-[532]$ |
| | 454; 508 | $\frac{5}{2}, \frac{3}{2}^-[532]$ | $\frac{5}{2}, \frac{3}{2}^-[532]$ |
| | 274; 406 | – | Omitted |
| | 527 | $\frac{7}{2}^-$ | $\frac{9}{2}, \frac{5}{2}^-[523]$ |
| | 897 | $\frac{5}{2}^-$ or $\frac{7}{2}^-$ | $\frac{5}{2}, \frac{1}{2}^-[530]$ |
| | 990 | $\frac{7}{2}^-$ | $\frac{7}{2}, \frac{1}{2}^-[530]$ |
| $^{155}$Gd | 235; 346 | $\frac{3}{2}^+; \frac{5}{2}^-$ | Omitted |
| | 287 | $\frac{9}{2}^-[532]$ | $\frac{3}{2}^-[532]$ |
| | 321, 393, 485 | $\frac{5}{2}^-[523]$ band | $\frac{5}{2}, \frac{7}{2}, \frac{9}{2}, \frac{3}{2}^-[532]$ |
| | 451 | $\frac{5}{2}^-[512]$ | $\frac{5}{2}^-[523]$ |
| | 556 | $\frac{7}{2}, \frac{1}{2}^-[530]$ | $\frac{7}{2}, \frac{5}{2}^-[523]$ |
| | 350 | $\frac{7}{2}, \frac{5}{2}^+[642]$ | $\frac{7}{2}, \frac{5}{2}^+[642]$ |
| | 489 | $\frac{5}{2}, \frac{1}{2}^+[400]$ | $\frac{5}{2}, \frac{1}{2}^+[660]$ |
| $^{153}$Sm | 362 | – | $\frac{5}{2}^+[642]$ |
| | 447 | $\frac{7}{2}, \frac{3}{2}^+[402]$ | $\frac{7}{2}, \frac{5}{2}^+[642]$ |
| | 524 | $\frac{5}{2}, \frac{1}{2}^+[400]$ | $\frac{5}{2}, \frac{1}{2}^+[660]$ |
| | 527, 730 | – | $\frac{9}{2}, \frac{13}{2}, \frac{5}{2}^+[642]$ |
| $^{155}$Dy | Ground band | [a] | $\frac{3}{2}^-[521]$ |
| | 423 | – | $\frac{7}{2}, \frac{3}{2}^-[532]$ |
| | 655; 409 | $\frac{3}{2}^+[651]$ | $\frac{3}{2}^+[651]$ |
| | 351 | – | $\frac{7}{2}, \frac{3}{2}^+[651]$ |
| | 558 | $l = 2$ or 3 | $\frac{5}{2}, \frac{3}{2}^+[651]$ |
| | 569 | $\frac{3}{2}^+$ | $\frac{1}{2}^+[660]$ |
| | 456 | $\frac{7}{2}^-(\frac{3}{2}^-[521], K+2)$ | $\frac{5}{2}, \frac{1}{2}^-[530]$ |
| | 557 | $\frac{5}{2}^-[512]$ | $\frac{5}{2}^-[512]$ |
| | 703 | $\frac{7}{2}^-[514]$ | $\frac{7}{2}, \frac{5}{2}^-[512]$ |
| $^{153}$Gd | Ground band | [a] | $\frac{3}{2}^-[521]$ |
| | 250 | $\frac{5}{2}^-$ or $l = 2$ | $\frac{5}{2}, \frac{3}{2}^-[532]$ |
| | 369 | $\frac{5}{2}^-$ or $\frac{7}{2}^-$ | $\frac{7}{2}, \frac{3}{2}^-[532]$ |
| | 195; 346 | $\frac{1}{2}^-; \frac{3}{2}^-$ or $\frac{5}{2}^-$ | Omitted |
| | 504; 316 | $\frac{3}{2}^+[651]$ | $\frac{3}{2}^+[651]$ |
| | 290 | – | $\frac{7}{2}, \frac{3}{2}^+[651]$ |
| | 442 | $\frac{5}{2}, \frac{1}{2}^+[400]$ | $\frac{5}{2}, \frac{3}{2}^+[651]$ |
| | 490 | (+) | $\frac{5}{2}, \frac{1}{2}^+[400]$ |
| | 221 | $\frac{11}{2}^+$ | No $\frac{11}{2}^+$ |
| $^{151}$Sm | 168 | $\frac{5}{2}^-$ | $\frac{5}{2}^-[523]$ |
| | 295 | $\frac{9}{2}^-, f_{7/2}$ | $\frac{7}{2}, \frac{5}{2}^-[523]$ |
| | 532 | $\frac{13}{2}^-, h_{9/2}$ | $\frac{9}{2}, \frac{5}{2}^-[523]$ |
| | 715 | – | $\frac{11}{2}, \frac{5}{2}^-[523]$ |
| | 423 | $\frac{11}{2}^-, f_{7/2}$ | $\frac{11}{2}, \frac{3}{2}^-[521]$ |
| | 502 | $\frac{11}{2}^-, h_{9/2}$ | $\frac{13}{2}, \frac{3}{2}^-[521]$ |
| | 416 | $\frac{5}{2}^-$ | $\frac{5}{2}, \frac{1}{2}^-[530]$ |
| | 307 | [a] | $\frac{3}{2}^-[402]$ |
| | 345 | [a] | $\frac{3}{2}^+[651]$ |
| | 324 | $\frac{7}{2}, \frac{3}{2}^+[651]$ | $\frac{7}{2}, \frac{3}{2}^+[651]$ |
| | 446 | $\frac{5}{2}^+[642]$ | $\frac{5}{2}, \frac{3}{2}^+[651]$ |
| | 627, 1054 | $\frac{15}{2}, \frac{19}{2}, \frac{3}{2}^+[651]$ | $\frac{15}{2}, \frac{19}{2}, \frac{3}{2}^+[651]$ |
| | 490 | $\frac{7}{2}^-$ | $\frac{7}{2}, \frac{3}{2}^+[402]$ |
| | 521 | $\frac{3}{2}, \frac{1}{2}^+[400]$ | $\frac{3}{2}, \frac{1}{2}^+[400]$ |

[a] Two contradictory proposals.

The structure of the low-energy excitations in $^{149}$Nd will be considered in more detail in another paper [51], where our lifetime measurements [12] in the nanosecond region together with the observations of [10] are compared with the model predictions.

Finally we summarize our discussion of the nuclei considered in Table V which includes the most important differences between the previous and present level assignments.

## 4. Summary

Comparison between the observations and calculations shows that the present model is capable of describing the properties of both the strongly and weakly deformed nuclei. In our opinion the $\frac{1}{2}^-[521]$ band does not have a strong vibrational character in the well-deformed nuclei under consideration. The present calculation has yielded systematic assignments for the states belonging to the $\frac{5}{2}^-[523]$ and $\frac{3}{2}^-[532]$ bands in $^{157}$Dy and in $^{155}$Gd. The different Coriolis coupling between these $f_{7/2}$ orbitals causes the clear difference in their level spacings, especially in the latter band, as Figs. 6 and 7 demonstrate. In addition, some members of the even-parity $\frac{5}{2}^+[642]$ and $\frac{1}{2}^+[660]$ side bands in $^{155}$Gd and $^{153}$Sm have been identified.

The ground states of $^{155}$Dy and $^{153}$Gd are confirmed as $\frac{3}{2}^-[521]$ states in distinction to $^{151}$Sm where the main components of the ground state come from the $f_{7/2}$ shell. For the other odd-parity states the model also produce a systematic description. The present study has increased our understanding of the low-spin positive-parity states, especially of the levels of the $\frac{3}{2}^+[651]$ side band in the weakly deformed nuclei. The attenuation of the Coriolis matrix elements has been previously found to depend on the polarization phenomenon of the nucleus. We propose that the average attenuation in a nucleus depends on its proton and neutron numbers as Fig. 1 shows. This systematic behaviour forecasts that the attenuation could appear also in the transitional $N = 87$ nuclei – at least in the lighter isotones.

For the description of the transitional odd-neutron nuclei close to the $N = 89$ shell the model parametrization – instead of the present choice – should be based on the fit to the single-particle states of the $N = 81$ and 83 nuclei. The promising results obtained hitherto lead us to assume that with such refitted parameters $V_0$ and $\lambda$ the present particle-rotor model is capable to describe even in more detail the structure of nuclei in that region.

## Acknowledgements

We wish to thank Prof. Antti Siivola, Prof. Pertti Lipas and Dr Timo Tuurnala for many enlightening discussions and critical reading of the

manuscript. Dr Sven Wahlborn has kindly made available the original computer programs used in our calculations. One of us (E.H.) is indebted to the Emil Aaltonen Foundation for financial support.

## References


1. Torres, J. P., Paris, P., Lecouturier, D. and Kilcher, P., Nucl. Phys. **A189**, 609 (1972).
2. Straume, O., Burke, D. G. and Thorsteinsen, T. F., Can. J. Phys. **54**, 1258 (1976).
3. Tuurnala, T., Siivola, A., Jartti, P. and Liljavirta, T., Z. Phys. **266**, 103 (1974).
4. Sen, P., Burman, C., Bakhru, H. and Howe, D., Z. Phys. **A274**, 343 (1975).
5. Løvhøiden, G. and Burke, D. G., Can. J. Phys. **51**, 2354 (1973).
6. Cook, W. B., Waddington, J. C., Burke, D. G. and Nelson, D. E., Can. J. Phys. **51**, 1978 (1973).
7. Nelson, D. E., Burke, D. G., Waddington, J. C. and Cook, W. B., Can. J. Phys. **51**, 2000 (1973).
8. Burde, J., Ginzburg, A. and Molchadzki, A., Phys. Rev. **C15**, 2187 (1977).
9. Cook, W. B., Johns, M. W., Løvhøiden, G. and Waddington, J. C., Nucl. Phys. **A259**, 461 (1976).
10. Pinston, J. A., Roussile, R., Börner, H., Koch, H. R. and Heck, D., Nucl. Phys. **A264**, 1 (1976).
11. Pinston, J. A., Roussille, R., Sadler, G., Tenten, W., Bocquet, J. P., Pfeiffer, B. and Warner, D. D., Z. Phys. **A282**, 303 (1977).
12. Hammarén, E., Liukkonen, E., Katajanheimo, R. and Tuurnala, T. (to be published).
13. Tuurnala, T., Z. Phys. **268**, 371 (1974).
14. Nilsson, S. G., Mat. Fys. Medd. Dan. Vid. Selsk. **29**, No. 16 (1955).
15. Nilsson, B., Nucl. Phys. **A129**, 445 (1969).
16. Hjorth, S. A. and Klamra, W., Z. Phys. **A283**, 287 (1977).
17. Guttormsen, M., Osnes, E., Rekstad, J., Løvhøiden, G. and Straume, O., Nucl. Phys. **A298**, 122 (1978).
18. Osnes, E., Rekstad, J. and Gjøtterud, O. K., Nucl. Phys. **A253**, 45 (1975).
19. Ogle, W., Wahlborn, S., Piepenbring, R. and Fredriksson, S., Rev. Mod. Phys. **43**, 424 (1971); Wahlborn, S., Nucl. Phys. **37**, 554 (1962); Wahlborn, S., Arkiv Fysik, **31**, 33 (1966).
20. Ehrling, G. and Wahlborn, S., Physica Scripta **6**, 94 (1972).
21. Rost, E., Phys. Lett. **26B**, 184 (1968).
22. Batty, C. J. and Greenlees, G. W., Nucl. Phys. **A133**, 673 (1969).
23. Almberger, J., Béthoux, R., Lindblad, Th., Lindén, G. and Wahlborn, S., AFI 1972 Ann. Rep. 3.7.2.
24. Rekstad, J. and Løvhøiden, G., Nucl. Phys. **A267**, 40 (1976).
25. Ragnarsson, I., Sobiczewski, A., Sheline, R. K., Larsson, S. E. and Nerlo-Pomorska, B., Nucl. Phys. **A233**, 329 (1974).
26. Götz, U., Pauli, H. C., Alder, K. and Junker, K., Nucl. Phys. **A192**, 1 (1972).
27. Baznat, M. I., Pyatov, N. I. and Chernej, M. I., Physica Scripta **6**, 277 (1972).
28. Nielsen, B. S. and Bunker, M. E., Nucl. Phys. **A245**, 376 (1976).
29. Wapstra, A. H. and Gove, N. B., Nuclear Data Tables **A9**, No. 4, 5 (1971).
30. Nilsson, S. G., Nucl. Phys. **55**, 97 (1964).
31. Abdurazakov, A. A., Adam, I., Gonusek, M., Gromov, K. Ya., Islamov, T. A., Rzhikovska, I. and Shtrusnyi, Kh., Izv. Acad. Nauk. SSSR, Ser. Fiz. **40**, 2089 (1976).
32. Tuli, J. K., Nuclear Data Sheets **13**, 493 (1974).
33. Bennett, M. J. and Sheline, R. K., Phys. Rev. **C15**, 146 (1977).
34. Bunker, M. E. and Reich, G. W., Rev. Mod. Phys. **43**, 348 (1971).
35. Prasad, K. G. and Nielsen, H. L., Physica Scripta **9**, 208 (1974).
36. Nybø, K. and Straume, O., Phys. Norv. **7**, 145 (1974).
37. Tjøm, P. O. and Elbek, B., Mat. Fys. Medd. Dan. Vid. Selsk. **37**, No. 7 (1969).
38. Adam, I., Baier, G., Gromov, K. Ya., Islamov, T. A., Ortlepp, Kh.-G., Tyrroff, Kh., Zherrmann, Z. and Shtrusnyi, Kh., Izv. Acad. Nauk. SSSR, Ser. Fiz. **39**, 1679 (1975).
39. Tuli, J. K., Nuclear Data Sheets **9**, 273 (1973).
40. Hjorth, S. A., Ryde, H., Hagemann, K. A., Løvhøiden, G. and Waddington, J. C., Nucl. Phys. **A144**, 513 (1970).
41. Torres, J. P., Paris, P. and Kilcher, P., Nucl. Phys. **A185**, 574 (1972).
42. Vylov, Ts., Gromov, K. Ya., Zelinski, A., Zuber, K., Zuber, Ya., Kuznetsov, V. V., Potempa, A. V. and Tominykh, V. I., Izv. Acad. Nauk. SSSR. Ser. Fiz. **36**, 2111 (1972).
43. Grotdal, T., Nybø, K., Straume, O. and Thorsteinsen, T., Phys. Norv. **8**, 33 (1975).
44. Meyer, R. A., Gunnink, R., Lederer, C. M. and Browne, E., Phys. Rev. **C13**, 2466 (1976).
45. Kroger, L. A. and Reich, C. W., Nuclear Data Sheets **15**, 409 (1975).
46. Tjøm, P. O. and Elbek, B., Mat. Fys. Medd. Dan. Vid. Selsk. **36**, No. 8 (1967).
47. Jaskola, M., Nukleonika **20**, 823 (1975).
48. Løvhøiden, G. (private communication).
49. Kroger, L. A. and Reich, C. W., Nuclear Data Sheets **10**, 429 (1973).
50. Smither, R. K., Bieber, E., von Egidy, T., Kaiser, W. and Wien, K., Phys. Rev. **187**, 1632 (1969).
51. Katajanheimo, R., Siivola, A., Tuurnala, T., Hammarén, E. and Liukkonen, E. (to be published).
52. Katajanheimo, R., Siivola, A., Tuurnala, T., Hammarén, E. and Liukkonen, E., Physica Scripta **19**, 247 (1979); Budzynsky, M., Buttsev, V. S., Gromov, K. Ya., Ion-Mikhay, R., Kalinnikov, V. G., Marupov, N. Z., Morozov, V. A., Muminov, T. M., Kholbaev, I. and Yakhim, M., Yaz. Fiz. **21**, 913 (1975).
53. Alikov, B. A., Budzynsky, M., Bedike, T., Vavrishchuk, Ya., Zhuk, V., Ion-Mikhay, R., Kuznetsov, V. V., Lizurei, G. I., Morozov, T. M., Muminov, T. M., Fominykh, M. I. and Kholbaev, I., Acta Phys. Pol. **B7**, 59 (1976).
54. Tuurnala, T. (private communication).
55. Løvhøiden, G., Hjorth, S. A., Ryde, H. and Harms-Ringdahl, L., Nulc. Phys. **A181**, 589 (1972).
56. Nelson, D. E., Burke, D. G., Cook, W. B. and Waddington, J. C., Can. J. Phys. **49**, 3166 (1971).
57. Harmatz, B., Nuclear Data Sheets **19**, 33 (1976).